

MAGNETIC INSTABILITIES IN STELLAR ATMOSPHERES

E.R.Priest

Applied Mathematics Department
The University, St.Andrews, Scotland.

ABSTRACT. The extensive theory for magnetohydrodynamic instability of a flux tube is briefly reviewed, together with its application to tokamaks and solar flares. In a star a single coronal loop whose footprints are anchored in the dense photosphere may become unstable to the kink instability when it is twisted too much. Magnetic arcades may also be subject to an eruptive instability when they are sheared too much. After the eruption the magnetic field closes back down by reconnection and continues to heat the plasma long after the impulsive phase. Global instability of a large part of the coronal magnetic field is also possible when the stored energy is too great.

1. INTRODUCTION

My aim in this review is to tell you some of the interesting lessons we have learnt from studying magnetic instabilities in tokamaks and solar flares. Hopefully, some of them may also be relevant to stellar flares. Twenty years ago it was recognised that typical magnetic structures on the Sun (with size 100,000 km and magnetic field a few hundred Gauss) contain enough energy (3×10^{25} J) to provide a flare. The main problem for theorists was to explain how to release the energy fast enough (over 10^3 sec). The time-scale for such release by ohmic dissipation is the diffusion time

$$\tau_d = \ell^2 / \eta, \quad (1.1)$$

where η is the magnetic diffusivity. With a typical length-scale (ℓ) of 10,000 km this gives times that are much too long (10^4 sec), and so it was realised that a current sheet is needed with a width of only 1 km or less. This led to the development of theories for fast magnetic reconnection at such sheets. Today we know much more about the solar flare, especially since the spectacular observations from Skylab and the Solar Maximum Mission. There are now many more constraints on the imagination of theorists, and the emphasis has shifted to trying to explain the basic magnetic instability that produces a flare. The observations have been reviewed in the books by Svestka (1976) and Sturrock (1980), while summaries of the theories can be found in, for example, Priest (1981,1982)

or Spicer and Brown (1981).

A typical large solar flare has three stages to its development. During the preflare phase (for $\frac{1}{2}$ hr) one sees a slow rise of a large magnetic flux tube (a filament or prominence), together with a soft X-ray brightening. At the rise phase (lasting for 5 mins - 1 hr) the flux tube suddenly erupts much more rapidly. There is a steep rise in H α emission from the chromosphere and in soft X-rays from the overlying coron \bar{a} , sometimes accompanied by a hard X-ray burst. The H α comes from two ribbons. During the main phase energy continues to be released, but the intensity declines slowly over an hour or a day. At the same time the H α ribbons separate and are joined by a rising arcade of hot loops up to 100,000 km high. The rise speed of the loops is at least 20 kms $^{-1}$ early in the event and only 0.5 kms $^{-1}$ later on. Their density and temperature are typically 10^{17} m $^{-3}$ and 2×10^7 K at first, falling to 10^{16} m $^{-3}$ and 5×10^6 K after a few hours. In regions where the magnetic field is weak (10G) a flare near a quiescent filament tends to be slow, long-lived and thermal, often with no H α emission at all. When the field is strong (500G) and complex near a plage (or active-region) filament the flare is violent, fast and non-thermal.

2. BASIC MHD INSTABILITIES OF A FLUX TUBE

2.1. Ideal Modes.

The theory of magnetic instabilities is now highly developed and has been clearly summarised by Bateman (1978) and Wesson (1978,1981), whom I shall follow here. The ideal modes grow fastest and have the magnetic field frozen to the plasma, whereas the resistive modes have lower thresholds for instability and allow the magnetic field to slip through the plasma in a narrow layer around a so-called resonant surface.

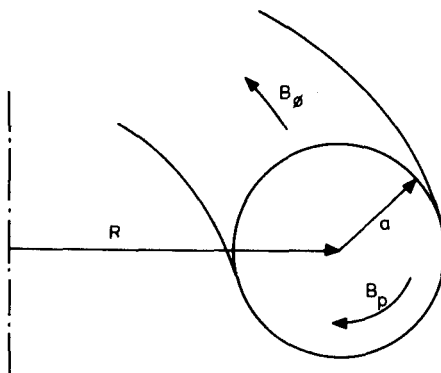


Figure 1. Notation for a curved flux tube.

Consider a magnetic flux tube of major radius R and minor radius a (both constant) with field components $B_p(r)$ (poloidal) and $B_\phi(r)$ (toroidal)

that depend on the distance (r) from the magnetic axis. Several useful quantities may be defined as follows. The *plasma beta* $\beta = 2\mu p/B^2$ is the ratio of plasma to magnetic pressure, and $\beta_p = 2\mu p/B_p^2$ is the corresponding ratio with the poloidal magnetic pressure. For a semicircular flux tube the amount by which a field line is twisted about the axis in going from one end of the tube to the other is $\Phi(r) = \pi R B_p / (r B_\phi)$. A related quantity is the *safety factor* $q(r) = r B_\phi / (R B_p) = \pi / \Phi$, which for a whole torus is the ratio of the wavelength of a field line to the major circumference ($2\pi R$) or, in other words, the number of turns that a field line makes around the major axis during one turn around the minor axis. Thus $q = 1$ would mean the field line twists once around the minor axis of a torus, whereas $q = 2$ would mean it undergoes half a twist. The inverse *aspect ratio* $\epsilon = a/R$ will be assumed much smaller than unity with $q \sim 1$ and $\beta \sim \epsilon^2$ (i.e. $\beta_p \sim 1$). The *shear* is $d/dr(q^{-1})$ and is a measure of the way the twist varies with radius. The electric current density along the flux tube is $j_\phi(r) \sim r^{-1} \partial/\partial r(r B_p)$, which takes the value $2B_p/(Rq)$ on the axis ($r = 0$). We shall consider a typical flux tube in which B_p increases with r from the axis while B_ϕ is roughly constant, j_ϕ decreases from a maximum and q increases from a minimum. As the tube is twisted up more, so j_ϕ increases and q falls in value.

A radial perturbation ξ proportional to $e^{i(m\theta - n\phi)}$ produces a shape like a single helix if $m = 1$ or a double helix if $m = 2$. The radius (r_s) where $q(r) = m/n$ is called a *resonant surface*, and is such that the orientation of the perturbation matches that of the field so that the crests and troughs of the helix follow the field lines.

To second order in ϵ there are no toroidal effects and the change in potential energy produced by the perturbation (assuming a vacuum outside the tube) is

$$\delta W_2 = \frac{\pi^2 B_\phi^2}{R} \left\{ \int_0^a \left[\left(r \frac{d\xi}{dr} \right)^2 + (m^2 - 1) \xi^2 \right] \left(\frac{n}{m} - \frac{1}{q} \right)^2 r \, dr + S_a \right\}, \tag{2.1}$$

or

$$\delta W_2 = \pi^2 R \int_0^a \left[B_1^2 + B_\theta (1 - nq/m) \frac{dj_\phi}{dr} \xi^2 \right] r \, dr, \tag{2.2}$$

where

$$S_a = \left[\frac{2}{q_a} \left(\frac{n}{m} - \frac{1}{q_a} \right) + (1+m) \left(\frac{n}{m} - \frac{1}{q_a} \right)^2 \right] a^2 \xi_a^2.$$

Here ξ_a is the surface perturbation and $B_1 = \nabla \times (\xi \times \frac{B}{r_0})$ is the magnetic field perturbation. When $\delta W < 0$ the equilibrium is unstable and otherwise it is stable.

Kink modes are driven by the current gradient and are *surface modes* in the sense that they distort the surface of the tube. They are the instabilities that arise at second order in ϵ and are potentially the strongest. It can be seen from (2.1) that they need $q_a < m/n$, so that the resonant surface is outside the tube. Also, the second term in (2.2) shows that it is the torque arising from the current gradient dj_ϕ/dr that drives the instability and that the destabilising region is inside the resonant surface (i.e. $q(r) < m/n$). Wesson (1978) has considered the

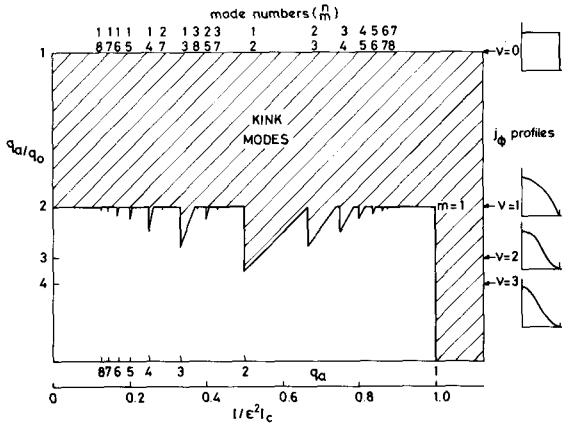


Figure 2. Kink instability diagram (Wesson, 1978).

current profile $j_{\phi} = j_{\phi 0} (1-r^2/a^2)^v$ for which the total current is $I = \pi a^2 j_{\phi 0} / (v+1)$ and the ratio of the q -values at the edge and axis of the tube is $q_a/q_0 = v + 1$. Figure 2 shows that when there is no shear ($q_a = q_0$) the tube is always kink unstable. At some value of v between 1 and 2.5 (depending on q) so that the current is sufficiently peaked, the mode becomes *stabilized by shear*. However, when $q_a < 1$ (the Kruskal-Shafranov boundary) the mode is always unstable. The effect of a potential or force-free plasma surrounding the tube is to provide some extra stability.

Internal (interchange) modes are driven by a pressure gradient and do not require a surface perturbation (i.e. $\xi_a = 0$). A resonant surface now lies inside the tube and the potential energy is of fourth order in ϵ with growth-rates smaller than those of the kinks by a factor ϵ . The modes with $m > 1$ are *localized around r_s* (i.e. $\xi = 0$ except near $q=m/n$) so that $\delta W_2 \approx 0$. In a cylindrical plasma they are unstable if

$$p' + r B_Z^2 / (8\mu) (q'/q)^2 < 0 \quad (\text{Suydam's criterion})$$

The first term is destabilizing when $p' < 0$ and the second term represents the *stabilizing effect of shear*. In a torus the curvature provides extra stability by multiplying p' by $(1-q^2)$ (Mercier's criterion), so that a negative pressure gradient is only destabilizing when $q_0 < 1$. Thus the internal modes occur below a diagonal line $q_0 = 1$ in Figure 1. For sufficiently high β these modes *balloon* (i.e. have a large variation along θ) on the outer surface of a curved tube where the curvature is unfavourable.

2.2. Resistive modes.

The inclusion of resistivity removes a constraint by allowing field-lines to break and rejoin in narrow layers around the resonant surfaces. The growth-times for the resulting instabilities lie between the diffusion time ($\tau_D = a^2/\eta$) and the Alfvén time ($\tau_A = a/v_A$), where $\tau_D \gg \tau_A$.

The resistive form of the kink mode is called a (surface) *tearing mode*. It is driven by the current gradient but now occurs when $q_a > m$ so that the resonant surface lies inside the tube. The Euler-Lagrange equation for (2.1) when $\eta = 0$ is

$$\frac{d}{dr} \left(r \frac{d}{dr} (r B_{r1}) \right) - m^2 B_{r1} - \frac{dj_\phi/dr}{(B_\phi/mr^2)(m-nq)} B_{r1} = 0, \quad (2.3)$$

where $B_{r1} = iB(m-nq)\xi/r$. This is also the equilibrium equation $\nabla \times (j \times r B) = \rho \hat{z}$ since the smallness of the growth-rate makes inertia negligible. The solutions to (2.3) starting at the axis and at infinity become singular at $r = r_s$, and so they need to be matched with those in the resistive layer. The result is that the mode is unstable when

$$\Delta' = \left[\frac{1}{B_{r1}} \frac{dB_{r1}}{dr} \right]_{r_s+\epsilon}^{r_s-\epsilon} > 0, \quad (2.4)$$

and the growth-time behaves like $\tau_d^{3/5} \tau_A^{2/5}$. For $m = 2$ the effect of twisting up a flux tube is to move to the right in Figure 3 and so cross the threshold first for tearing ($q_a = 2$) and then, as the resonant surface crosses $r = a$, for kinking ($q_a = 2$). (One may be tempted to equate the crossings of such thresholds with the onset of the preflare phase and rise phase of a flare, but we shall see below that tokamak phenomena are not so simple and require nonlinear theory for their interpretation.) The lower boundary in Figure 3 appears because of shear stabilization when q_a/q_0 is large enough. A similar figure is obtained for $m = 3$, but modes with $m > 3$ are stabilized because of the tension term ($-m^2 B_{r1}$) in (2.3).

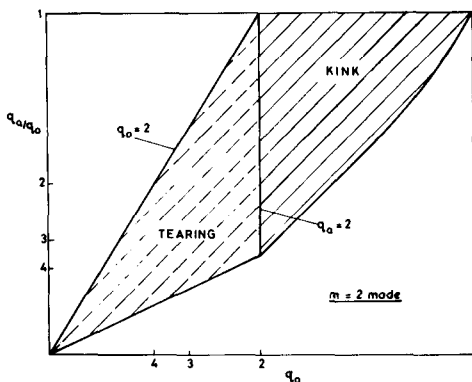


Figure 3. Instability of $m = 2$ mode (Wesson, 1978).

The *resistive interchange* (or resistive g) modes are the resistive form of the internal modes with $m > 1$ and have growth times of order $\tau_d^{1/3} \tau_A^{2/3}$. The effect of increasing the shear is to localize the modes and reduce their growth-rate. They are unstable if

$$(-p') \left\{ q^2 - 1 + \frac{q^3 q'}{r^3} \int_0^r \frac{r^3}{q^2} + \frac{2R^2 r^2}{B_\phi} (-p') dr \right\} < 0,$$

and so under normal conditions ($p' < 0$, $q' > 0$) they require $q_0 < 1$. Increasing β provides more stability by changing the solution in the resistive layer and modifying the instability criterion to $\Delta' > \Delta'_c$, where Δ'_c increases with β . The threshold for stability of $m = 2$ is moved to the right from $q_0 = 2$ in Figure 3 and the mode is completely stabilized when $\Lambda > 60$ ($\Lambda > 10$ for $m = 3$), where $\Lambda = \beta^{5/6} \epsilon^2 (\tau_d / \tau_A)^{1/3}$. However, resistive ballooning modes appear. The $m = 1$ internal resistive kink mode becomes unstable when $q_0 < 1$. As the twist is increased so the flux tube becomes tearing mode unstable first with $i\omega \sim \eta^{3/5}$, then it passes through a region where $i\omega \sim \eta^{1/3}$ and finally it becomes unstable to the ideal mode. The importance of other resistive effects in enhancing the dissipation in flares has been debated by Spicer (1977) and Van Hoven (1981).

3. APPLICATION TO TOKAMAKS.

A standard tokamak is a torus with $q \sim 1$, $\epsilon \ll 1$ and $\beta \sim \epsilon^2$ so that $a \ll R$, $B_p \ll B_0$ and $p \sim B_p^2 / (2\mu)$. The aim is to confine plasma at $T \sim 15 \text{ keV}$ (10^8 K), $n \sim 10^{20} \text{ m}^{-3}$, $B \sim 20\text{--}100 \text{ kG}$, $\beta \sim 5\%$ for a time $\sim 1 \text{ sec}$. At present the values reached are $\beta \sim 2\%$ and $\tau \sim 0.1 \text{ sec}$. In contrast, a reversed field pinch has $B_p \sim B_0$ with a higher β (10%) but (so far) a lower confinement time (10^{-2} sec). Three phenomena appear to be produced by MHD instabilities in tokamaks as follows.

Mirnov oscillations show up with magnetic pickups as a small regular vibration at several values of $m > 1$. They are due to resistive modes near the $q = m$ surfaces that have saturated nonlinearly to a steady state containing islands. Finite Larmor radius effects cause the steady helical structure to rotate around the torus.

Sawtooth oscillations with a period of a few milliseconds appear in the soft X-ray emission from the core of the plasma. They are relaxation oscillations due to nonlinear effects of the internal resistive $m = 1$ mode (Figure 4). The ohmic heating (σE^2) driven by the applied electric field (E) slowly concentrates the current towards the axis, because the heating raises the temperature, the conductivity ($\sigma \sim T^{3/2}$) and therefore the current ($j \sim \sigma E$). When q_0 falls below 1 the $m = 1$ resistive mode occurs rapidly and creates a magnetic island with $q > 1$. This grows by reconnection and eventually displaces the old island creating a new stable state. The true B does not reverse sign, but Figure 4 refers to the magnetic field you would see looking at angle such that the line-of-sight field vanishes at the radius where $q = 1$.

Disruptive instability is the most dramatic event in tokamaks. When the current is so large that q_0 falls below about 2.5 the $m = 2$ oscillations grow rapidly over a few milliseconds, hard X-rays are emitted, and the soft X-ray emission falls, followed by a rapid collapse of the current. The explanation is rather controversial (like that of flares!). One possibility is the nonlinear destabilization of the $m = 3$, $n = 2$ mode by the $m = 2$ mode (Waddell et al, 1979), producing many magnetic islands with ergodic fields and a rapid escape of heat from the core. Alternatively, it may be due to a magnetic catastrophe. Usually, the tearing mode

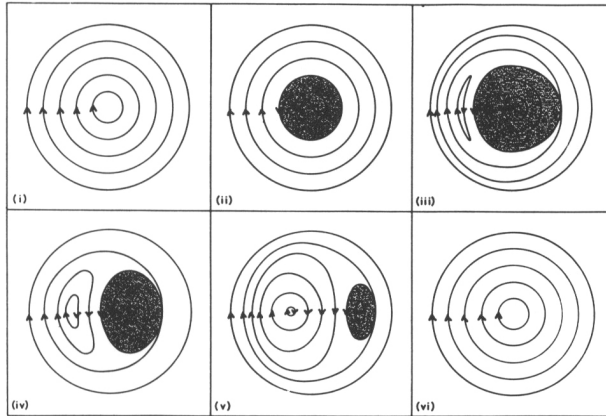


Fig. 4. Model for sawtooth oscillations (Wesson, 1980).

is self-stabilizing with a saturated state that reduces the current gradient (j_{ϕ}'), but if the current is too large Sykes and Wesson(1981) and Wesson et al(1982) have demonstrated that the saturated equilibrium no longer exists. The current profile $j_{\phi}(r)$ is modified by the $m = 1$ and $m = 2$ modes, whose islands flatten it near the resonant surfaces at $q(r) = 1$ and $q(r) = 2$. The widths (ω) of the islands are determined by $\Delta'(\omega) = 0$, with Δ' given by (2.4), B_{r1} given by (2.3) and j_{ϕ}' in (2.3) modified by the presence of the islands. As the current grows so the island widths grow until, at some critical width, $\Delta'(\omega) = 0$ no longer has a solution.

Lessons that may be learnt for astrophysics from tokamak studies include the following. The details of the magnetic structure (B_{θ}/r) and $j_{\phi}(r)$ are important for determining the relevant instability. The resistive modes occur at lower thresholds than the ideal ones, but they are not necessarily destructive since they may instead produce gentle oscillations (Mirnov or sawtooth). It is crucial to study the nonlinear development of any instability to see whether it saturates (sawtooth) or grows explosively (disruptions).

4. SOLAR FLARES.

4.1. Loop configuration.

The ideal kink instability of a force-free loop has been studied by several authors (Raadu, 1972 ; Hood and Priest, 1979. ; Van Hoven et al, 1981 ; Einaudi and Van Hoven, 1981) using different forms for ξ and different equilibrium fields. We saw in §2.1 that a tube of uniform twist is always unstable, but in the Sun there is a most important extra stabilizing influence, namely *line-tying*, since the feet of the loop are anchored in the dense photosphere. Such a line-tied perturbation takes the form

$$\xi = (\xi_r, -B_{0z}\xi_\theta/B_0, B_{0\theta}\xi_\theta/B_0) e^{i(\phi + \omega t)}$$

in a cylindrical geometry such that $\xi_\theta \cdot B_0 = 0$. The equation of motion is

$$\rho_0 \partial^2 \xi / \partial t^2 = j_1 \times B_0 + j_0 \times B_1,$$

where $j = \nabla \times B / \mu$ and $B_1 = \nabla \times (\xi \times B_0)$, subject to the conditions that ξ vanish as $r \rightarrow \infty$ and at the ends ($z = \pm L$) of the loop. This gives a pair of partial differential equations for $\xi_r(r, z)$ and $\xi_\theta(r, z)$, whose numerical solution (Hood and Priest, 1981) gives stability when the tube is slightly twisted and instability when the twist (ϕ) exceeds 2.5π (i.e. $q < 0.4$). The effect of pressure gradients and line-tying has been included by Hood and Priest (1979) and Hood, Priest and Einaudi (1982), who obtain analytical, line-tied solutions for a magnetohydrostatic loop with a sharp boundary. They find that stretching or twisting it eventually makes it unstable.

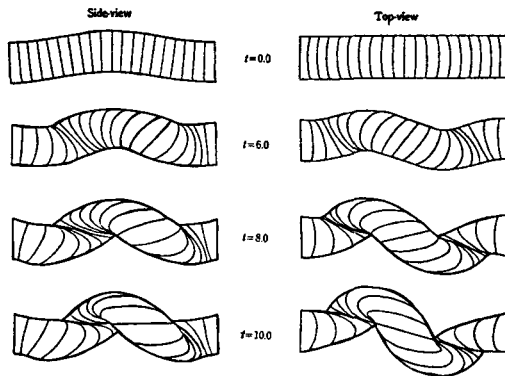


Figure 5. Kinking of a flux tube (Sakurai, 1976).

In future, it is important to study several other effects due to the resistive modes, shear stabilization and the curvature and non-uniform cross-section of a loop. A start has been made on following the non-linear development by Sakurai (1976). He considers an infinitely long cylinder of uniform current or a force-free field and simulates line-tying roughly by requiring that the axial wavenumber (k) be π/L . His numerical solutions (Figure 5) show how the flux tube rises and twists up. Tubes with a weak twist develop strong helical kinks and rise less than those with strong twist because of the stabilizing tension force from the axial field.

4.2. Magnetic Arcades.

A coronal magnetic field evolves passively through a series of (largely) force-free equilibria and stores more and more energy in response to the motions of its photospheric footpoints until it becomes unstable. This point of instability may be found by seeking multiple equilibrium solutions to the same photospheric boundary conditions on the plane $y = 0$ (Low, 1977 ; Birn et al, 1978; Priest and Milne, 1980).

For a magnetic field of the form

$$\mathbf{B} = (\partial A/\partial y, -\partial A/\partial x, B_z(A)) \tag{4.1}$$

the force-free field equation ($\mathbf{j} \times \mathbf{B} = 0$) reduces to

$$\nabla^2 A = -B_z \frac{dB_z}{dA},$$

where the horizontal displacement of the footpoints from the x-axis in the z-direction is $d(x) = B_z \int dx/B_z$ and $B_y(x,0)$ is prescribed. Good progress has been made so far, but mainly with the case when B_z rather than the footpoint displacement (d) is prescribed. In particular, Heyvaerts et al (1980) have discovered at least three solutions and therefore the possibility of jumping violently from one to another.

Magnetic stability of arcade equilibria has been tested directly by Van Tend and Kuperus (1978), Hood and Priest (1980) and Birn and Schindler (1981). Hood and Priest included line-tying but were unable to find a perturbation that destabilizes a simple arcade with a field of the form (4.1) and no magnetic island above the photosphere. This led them to consider arcade fields with the axis (an O-type neutral point in the x-y plane) a distance d above the photosphere ($y=0$) and the field lines twisted about this axis by an amount Φ as they ascend from the photosphere and return to it again. Such arcades are stable when d and Φ are small but become unstable when Φ or d exceed critical values. Thus, the eruption of an arcade may be due to a spontaneous MHD instability when Φ or d are too big or due to a resistive instability below the filament when d is too large. Alternatively, it may be triggered by some extra effect such as : emerging flux, which can push the filament up and tear away some of the overlying field lines or lower the tearing mode time by creating a small region of enhanced resistivity and initiating a large-scale reconnection (Heyvaerts et al, 1977); a thermal instability in the filament, which causes the plasma to expand and makes the tube rise until the critical d is reached; a fast magnetoacoustic wave, which can couple to and trigger tearing with a faster growth-rate than normal (Sakai and Washimi, 1982).

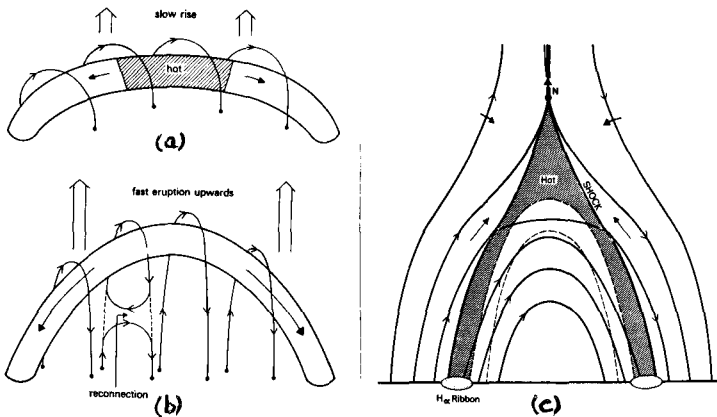


Figure 6. Overall behaviour of a flare.

4.3. Main phase.

The overall behaviour of a solar flare is indicated in Figure 6. First of all a magnetic flux tube rises slowly and stretches out the field lines of the overlying arcade. Then the rapid eruption is triggered and the field below the flux tube starts to tear. Later on (Figure 6c in a cross-section across the arcade), the field lines that have been dragged open by the eruption continue to close down and re-connect at the neutral point N. This rises and trails behind it a pair of slow MHD shock waves, which heat the plasma and create hot loops (Cargill and Priest, 1982). This process of line-tied reconnection has been simulated numerically by Forbes and Priest (1982) with typically $\beta = 0.1$ and $\tau_d/\tau_A = 10^3$. They find that the field lines that are being stretched out by the erupting flux tube tear first near the base. In the nonlinear phase the flows build up to a large fraction of the Alfvén speed and a quasi-steady state of Petschek-like reconnection develops with the X-type neutral point (N) rising and a region of closed loops being created below N. Above N a plasmoid is ejected and the sheet thins. Eventually, it tears again creating a pair of O and X neutral points (Figure 7). Reconnection at the upper X dominates and the O is rapidly shot down to coalesce with the lower X. This process can repeat and may be an efficient means of accelerating particles.

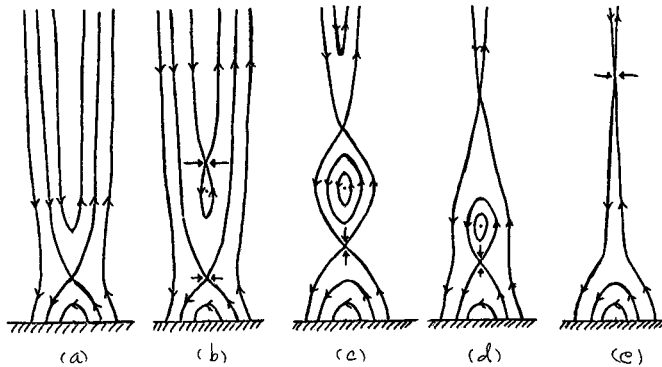


Figure 7. Creation and annihilation of neutral point pairs during the main phase of a flare (Forbes & Priest, 1982).

5. STELLAR FLARES.

Stellar flares may be caused by similar instabilities to the ones we have described for solar flares. The energy of a flare should scale like $W = L^3 B^2 / (2\mu)$ in terms of the local magnetic field (B) and the size (L) of the magnetic region, while the time-scale for energy release is just $\tau \approx L / (0.01 V_A)$, where $V_A = B / (\mu\rho)^{1/2}$, and the pressure is $p \approx B^2 / (2\mu)$, although on the Sun itself this scaling is only rough, since one has a wide range in W , τ and p . On a star one may find instability when the plasma pressure builds up so much that it cannot be contained by the

magnetic field, or when the density builds up so much that it cannot be supported against gravity by a sheared field (Rayleigh-Taylor instability). Again, if a giant flux tube erupts by magnetic buoyancy in a violent manner it may produce the giant equivalent of the tiny X-ray bright points seen on the Sun.

A solar flare is caused by the magnetic instability and subsequent reconnection of a *local* magnetic region. But stellar flares may instead arise when *global* magnetic equilibrium breaks down. Several solutions have been presented for the global magnetic field in the corona of a star. Consider an axisymmetric field

$$\mathbf{B} = \frac{1}{r \sin \theta} \left(\frac{\partial A}{\partial \theta} \hat{r} - \frac{\partial A}{\partial r} \hat{\theta} + B_{\phi}(A) \hat{\phi} \right)$$

with pressure $p = p_0(A) \exp - \int_r^R GM/(RTr^2) dr$. Then the force balance equation $(\mathbf{J} \times \mathbf{B} - \nabla p - \rho \mathbf{G} = \mathbf{0})$ reduces to the basic equation

$$\frac{\partial^2 A}{\partial r^2} + \frac{\sin \theta}{r^2} \frac{\partial}{\partial \theta} \left(\frac{1}{\sin \theta} \frac{\partial A}{\partial \theta} \right) + B_{\phi} \frac{dB_{\phi}}{dA} + 4\pi r^2 \sin^2 \theta \frac{\partial p}{\partial A} = 0. \tag{5.1}$$

Analytical solutions have been discovered by Uchida and Low (1981) with $B_{\phi} = 0$ and $p = Q(r)A$, so that (5.1) reduces to a linear equation with solutions of the form $A = r^2 u(r) \sin^2 \theta$. In particular, they discuss fields that are dipolar at the surface and uniform at large distances, and they consider the effect of different mass loadings.

When the pressure gradient and gravitational forces are negligible, (5.1) describes a *force-free* field. Raadu (1972) started with a quadrupole field and calculated the effect of increasing B_{ϕ} due to differential rotation of the footpoints. He found that the poloidal field lines expand outwards to provide an extra magnetic tension to contain the magnetic pressure of B_{ϕ} . The magnetic energy increases by 25% in one rotation. Later, Milsom and Wright (1976) considered a particular form of $B_{\phi}(A)$ such that $B_{\phi} dB_{\phi}/dA = \alpha A^n$, with $n = 4$ for instance. They matched numerically the dipole surface field to a dipolar field at infinity of the form $A = A_{\infty} r^{-1} \sin^2 \theta$, which is only possible when $n > 3$. As α increases so the toroidal field (B_{ϕ}) increases and the field distorts until at a critical value of $\alpha \approx 0.8$, A_{∞} becomes infinite, so that the field cannot be contained any longer and blows open. A similar feature should be present if the coronal pressure increases too much due to, for instance, too much heating. A similar effect has been demonstrated analytically by Browning and Priest (1973) by putting $B_{\phi} = B_0 A$ and $A = A_0(r) \sin^2 \theta$, so that (5.1) reduces to

$$d^2 A_0 / dr^2 + (B_0^2 - 2r^{-2}) A_0 = 0,$$

with solution

$$A_0 = C_1 / (\lambda r) \cos(\lambda r + C_2) + C_1 \sin(\lambda r + C_2).$$

She supposes that a stellar wind makes the field radial at some radius s_0 and imposes a dipole field at the surface. Starting with a potential field, the effect of differential rotation in twisting up the field is considered by increasing λ . The field lines expand up to a maximum λ

of 1.4 s^{-1} , above which a physically reasonable field no longer exists, since field lines detached from the star appear near the equator which would be pulled out by the stellar wind. The same effect is present with a quadrupolar field or an increasing pressure ($p = p_0 A$).

6. CONCLUSION.

Depending on the detailed magnetic structure, there is a rich variety of ways in which a magnetic field can go unstable due to either an ideal or a resistive mode. It is essential to study the nonlinear development of such instabilities: they need not always be fatal since they may easily be saturated and reach new equilibria rather than growing explosively. We have learnt much about solar flares from the wonderful observations of Skylab and SMM - what riches would be in store for us if we could view their stellar counterpart with as much clarity. Solar flares are due to an eruptive instability of a loop or arcade and the subsequent reconnection process as the magnetic field closes back down. Stellar flares may be due to a similar process or due to a lack of global equilibrium. However, there is a need to study such equilibria and their stability in much more detail.

REFERENCES.

- Bateman, G.: 1978, *MHD instabilities*, MIT Press.
- Birn, J., Goldstein, H. and Schindler, K.: 1978, *Solar Phys.* 57, 81.
- Birn, J. and Schindler, K.: 1981, Ch.6 of *Solar flare MHD* (ed. E. Priest), Gordon and Breach.
- Browning, P. and Priest, E.: 1983, preprint.
- Cargill, P. and Priest, E.: 1982, *Solar Phys.* 76, 357.
- Einaudi, G. and Van Hoven, G.: 1981, *Phys. Fluids* 24, 1092.
- Forbes, T. and Priest, E.: 1982, *J. Plasma Phys.* 27, 157.
- Heyvaerts, J., Lasry, J., Schatzman, M., Witomsky, G.: 1980, *Lecture Notes Math.* 782, 160.
- Heyvaerts, J., Priest, E. and Rust, D.: 1977, *Ap. J.* 216, 123.
- Hood, A. and Priest, E.: 1979, *Solar Phys.* 64, 303.
- Hood, A. and Priest, E.: 1980, *Solar Phys.* 66, 113.
- Hood, A. and Priest, E.: 1981, *Geophys. Astrophys. Fluid Dynamics* 17, 297.
- Hood, A., Priest, E. and Einaudi, G.: 1982, *Geophys. Astrophys. Fluid Dynamics*, 20, 247.
- Low, B. C.: 1977, *Ap. J.* 212, 234.
- Milson, F. and Wright, G.: 1976, *Mon. Not. Roy. Astron. Soc.* 174, 307.
- Priest, E.: 1981, *Solar Flare MHD*, Gordon and Breach.
- Priest, E.: 1982, *Fund. Cosmic Phys.* 8.
- Priest, E. and Milne, A.: 1980, *Solar Phys.* 65, 315.
- Raadu, M.: 1971, *Astrophys. Space Sci.* 14, 464.
- Raadu, M.: 1972, *Solar Phys.* 22, 425.
- Sakai, J. and Washimi, H.: 1982, *Ap. J.*, in press.
- Sakurai, T.: 1976, *Pub. Astron. Soc. Japan* 28, 177.
- Spicer, D.: 1977, *Solar Phys.* 53, 305.

- Spicer, D. and Brown, J. : 1981, *The Sun as a star* (ed. S. Jordan), Ch. 18.
- Sturrock, P. : 1980, *Solar flares*, Colo. Ass. Univ. Press.
- Svestka, Z. : 1976, *Solar flares*, D. Reidel.
- Sykes, A. and Wesson, J. : 1981, *Plasma physics and controlled nuclear fusion research*, 1, 237.
- Uchida, Y. and Low, B. C. : 1981, *J. Astrophys. Astron.* 2, 405.
- Van Hoven, G. : 1981, Ch. 4 of *Solar flare MHD* (ed. E. Priest), Gordon and Breach.
- Van Hoven, G., Maa, S., Einaudi, G. : 1981, *Astron. Astroph.* 99, 232.
- Van Tend, W. and Kuperus, M. : 1978, *Solar Phys.* 59, 115.
- Waddell, B., Carreras, B., Hicks, H., Holmes, J., Lee, D. : 1978, *Phys. Rev. Letters* 41, 1386.
- Wesson, J. : 1978, *Nuc. Fusion* 18, 87.
- Wesson, J., Sykes, A. and Turner, M. : 1982, preprint.

ACKNOWLEDGEMENT.

The author is most grateful to J. Wesson for many helpful discussions and to the staff of Culham Laboratory for their hospitality during his stay.

DISCUSSION

Nordlund: I will concentrate my question on your description of two-ribbon flares. I think it is fairly well established that the velocities we see when the loops rise are to a large extent apparent because successive loops brighten rather than a single loop brightening. A second point with regard to the instabilities you talked about, in the loop case we have found that the resistive instabilities came before the ideal ones. So don't you suspect that would be also the case in the arcade case? You just treated the ideal case.

Priest: I will take the first point first. Certainly it is believed that the rise of the loops as observed does not represent a bodily rise of the plasma. Rather it represents the fact that the neutral point at which reconnection takes place is rising. So, as the magnetic field closes back down, you are forming new loops one on top of the other. With regard to the second point, I believe that we are only beginning to take account of the experience of the laboratory plasma physicists and, as a result, so far people have only taken the ideal instabilities into account in giving rise to two-ribbon flares. As I mentioned I think we certainly must put the effects of resistivity into these calculations. That is by no means a trivial matter however and as I have pointed out, resistive modes do not always give rise to explosive behaviour. They just give rise to rather mild oscillations instead.

Stencel: A question concerning your numerical simulation of reconnection with Forbes. Have you considered the amount of mass ejected upward as a function of magnetic intensity?

Priest: No, we have not. These simulations have only been carried out fairly recently and we have not got as far as that. But it is something well worth doing.

Uchida: The numerical calculation which you made forming a magnetic island is very interesting. Sato and Hayshi have also shown numerically that forced reconnection is very efficient. In your calculation is mass sucked out of the region or is it pressed into the region? This is a boundary condition problem.

Priest: The Sato and Hayshi calculation does not start with equilibrium. Rather they impose a flow from the sides and then investigate the structure of the reconnection. Our simulation, which numerically is very similar to theirs, starts out with an equilibrium and then follows the development of the tearing mode into its non-linear phase. The important effect which we put in is the effect of line-tying on the base and this we regard as the most important aspect of our work.